Optimizing Central Electron Bernstein Wave Deposition via O-X-B Double Mode Conversion in the TCV Tokamak

L. Curchod[1], A. Mueck[1,3], A. Pochelon[1], R. Behn[1], S. Coda[1], T.P. Goodman[1], H.P. Laqua[2], J.-M. Moret[1], I. Pavlov[1], L. Porte[1], V.S. Udintsev[1] and the TCV team[1]

[1] *Ecole Polytechnique Fédérale de Lausanne (EPFL), Centre de Recherches en Physique des Plasmas, Association EURATOM-Confédération Suisse, CH-1015 Lausanne, Switzerland*

[2] *Max-Planck-Institut für Plasmaphysik, EURATOM Assoziation, D-17491 Greifswald*

Introduction The electron Bernstein wave (EBW) is an electrostatic mode propagating without upper density limit [1]. The study of EBWs is therefore of great interest in the prospect of extending fusion experiments operation to high-density heated plasmas. Electron Bernstein wave heating (EBWH) is of particular relevance in low to medium magnetic field devices where the cutoff frequency prevents standard electron cyclotron resonant heating and current drive (ECRH and ECCD) above a density threshold by the appearance of an evanescent layer at the edge of the plasma. EBWH via the ordinary-extraordinary-B (O-X-B) double-mode-conversion of microwaves injected from the low-field-side (LFS) of the discharge was proposed in [2]. The O-X conversion takes place at the O-mode cutoff and has a transmission function [3]

$$T_{\mathrm{ox}}(N_\perp, N_\parallel) = \exp\left\{-\pi k_0 L_n \sqrt{\frac{Y}{2}}\left[2(1+Y)(N_{\parallel\mathrm{opt}} - N_\parallel)^2 + N_\perp^2\right]\right\} \tag{1}$$

defining an O-X-conversion-efficiency angular window centered on the optimum parallel refractive index $N_{\parallel\mathrm{opt}}$ equivalent to an optimum injection angle and giving maximum conversion efficiency (for a given $N_\perp$). In Eq. (1) all quantities have to be evaluated at the conversion point: the components of the refractive index perpendicular $N_\perp$ and parallel $N_\parallel$ to the magnetic field, the density scale length $L_n = \frac{n_e}{\nabla n_e}$ normalized to the wave-vector k_0 of the pump wave of frequency ω and $Y = \frac{\omega_{ce}}{\omega}$ with ω_{ce} the electron cyclotron frequency. The electron density must be above O-mode cutoff density for T_{ox} to be non-zero, and L_n has to be small, that is the electron density gradient must be steep at the conversion point (typically close to the edge of the plasma) to achieve a large conversion window. In hot plasmas the X-B conversion automatically occurs at the upper hybrid resonant (UHR) layer with $\sim 100\%$ efficiency. The application of the O-X-B scheme for EBW heating in standard-aspect-ratio tokamaks was demonstrated for the first time by injecting 2$^{\mathrm{nd}}$ harmonic O-mode (O2 at 82.7 GHz) EC power in plasmas of the Tokamak à Configuration Variable (TCV, aspect-ratio $R/a \sim 3.6$, toroidal field $1.2\ \mathrm{T} < B_\varphi < 1.5\ \mathrm{T}$) [4]. In TCV, the conditions for a large O-X conversion window are met at the edge of overdense ($n_e \geq 10 \cdot 10^{19}\ \mathrm{m}^{-3} > n_{e,\mathrm{cutoff,O2}}(82.7\ \mathrm{GHz}) \sim 8.7 \cdot 10^{19}\ \mathrm{m}^{-3}$) high-confinement mode (H-mode) plasmas with ELM-free/ELMy periods, low $q_{95} = 2.2 - 2.4$, high triangularity $\delta = 0.5 - 0.6$ and medium elongation $\kappa = 1.8$ (high plasma current $I_p \simeq 420$ kA). In this paper, results of EBW emission (EBE) experiments in TCV are presented along with initial EBW equatorial injections yielding central power deposition determined with "slope-change" methods.

Electron Bernstein Wave Emission In TCV In TCV, 2nd harmonic electron cyclotron emission (ECE) from oblique directions is observed with a recently commissioned equatorial antenna [5] connected to the radiometer of the LFS ECE system. The antenna is geometrically identical to the 4 upper lateral and 2 equatorial launchers for the EC power at the 2nd harmonic: its mirror is steerable in 2 directions (named "toroidal" and "poloidal" angles $(\varphi_\tau, \varphi_\pi)$). In particular EBWs naturally excited with $N_\parallel = N_{\parallel \mathrm{opt}}$ in the plasma can leave it at densities above the O-mode cutoff density via the B-X-O double-mode-conversion backward process. The horizontal component of the emitted oblique O-mode is detected with this antenna. As an initial assumption, the X-O and O-X conversions are supposed to be symmetrical with the same transmission function T_{ox}, as given in Eq. (1). The theoretical emission optimum angle is predicted at $(\varphi_\tau, \varphi_\pi) = (129.4°, 35.1°)$ with simulations of the non-relativistic ray-tracing code ART for the injection. Then scans of the poloidal and toroidal angles of the antenna with respectively the toroidal and poloidal angles kept constant are carried out around the calculated optimum on a shot to shot basis to check the presence of an optimum viewing angle for the EC emission from overdense plasmas. The amplitude of the signal (normalized to the signal before the plasma cutoff onset) at high density ($n_e = 12 \cdot 10^{19}$ m^{-3}) exhibits a maximum versus both angles (Fig. 1) and for all emission frequencies measured by the radiometer. Gaussian fits on the data situate the experimental emission optimum angles at $(\varphi_\tau, \varphi_\pi) = (134.2°, 41.5°)$. The discrepancy between the experimental and the simulated angular optima is larger for EBE ($\sim 7°$ poloidally) than for EBWH experiments ($\sim 3°$) in similar conditions [4]. This could be the signature of the forward/backward asymmetry of the O-X conversion revealed by recent theoretical developments [6]:

$$T_{\mathrm{ox}}(\mathbf{B}) = T_{\mathrm{xo}}(-\mathbf{B}) \qquad (2)$$

With the antenna viewing in the experimental optimum direction, standard oblique ECE is measured at low density. When the density increases in an ELM-free period, the left-circularly-polarized component of the elliptically-polarized oblique

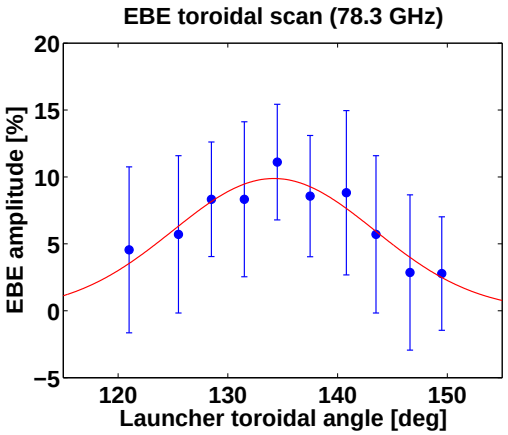

Figure 1: Amplitude of overdense ($n_e = 12 \cdot 10^{19}$ m^{-3}) signal vs. toroidal antenna viewing angle φ_τ and gaussian fit. A maximum of emission is found, as in function of the poloidal angle φ_π. Large error bars come from the low signal/noise ratio.

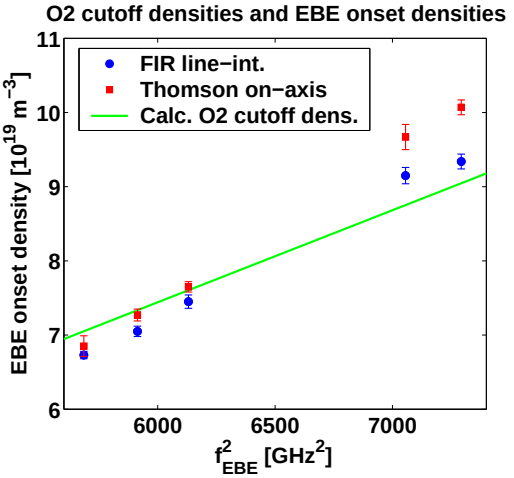

Figure 2: EBE onset central densities from a line-integrated far infrared interferometer (FIR, blue •) and Thomson scattering (red ■) compared to the calculated O2 cutoff.

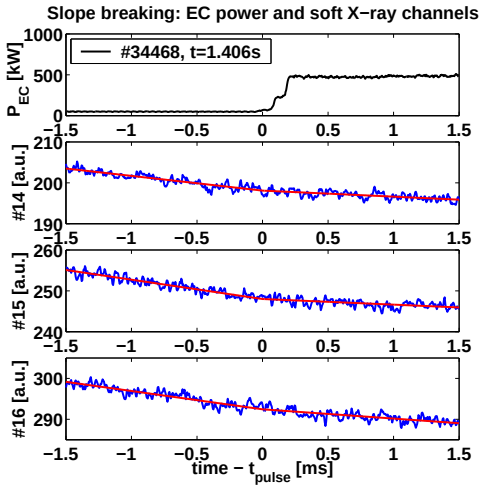

Figure 3: Onset of EC power pulse and soft X-ray signals (blue, DMPX channels #14 – 16). Linear fits (red lines) are carried out on the 64 soft X-ray flux time-traces 1.5 ms before and after the beginning of the heat pulse to calculate the slope difference.

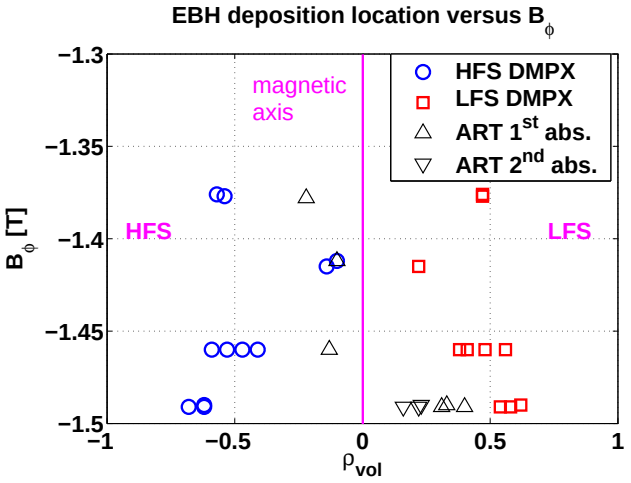

Figure 4: EBH deposition location from a "slope-break" method applied on DMPX signal from chords viewing in the HFS (blue ○) and LFS (red □) versus toroidal magnetic field B_φ. The EBW deposition location is shifted from the LFS to the HFS through the center as the magnetic field B_φ amplitude is decreased. ART simulations (△) show a secondary deposition location (▽) for high $|B_\varphi|$.

O-mode emission gets in cutoff and the signal is reduced. If the density goes on rising, a clear increase in the signal is measured in all frequency channels. As expected for EBE, the onset density of this overdense emission is different for the different frequencies and matches the theoretical O2 cutoff densities $n_{e,\mathrm{cutoff,O2}}(\omega_{\mathrm{O2}}) = \frac{\omega_{\mathrm{O2}}^2\, m_e\, \varepsilon_0}{e^2}$ within 5 to 10% (Fig. 2). The fact that the density was measured in the center and not at the conversion point can explain this discrepancy.

Initial Equatorial EBW heating studies First EBWH experiments in TCV were performed with a poloidal oblique launch in H-mode plasmas in the upper half of the tokamak ($Z_{\mathrm{axis}} \sim 20$ cm) [4]. The deposition location was determined at the edge ($0.7 < \rho_\psi < 0.8$) with fast Fourier transform (FFT) of the signal of a duplex 64-wire-chamber proportional soft X-ray detector (DMPX) with high spatial and temporal resolutions. The target discharge is moved down in front of the 2 equatorial launchers of TCV ($Z_{\mathrm{axis}} \sim 2$ cm) which favours a central power deposition. The O2 EC power from 1 or 2 gyrotrons is modulated between 0 and 500 kW at 182 Hz with 50% duty-cycle. B_φ is varied between -1.49 T and -1.37 T to radially shift the EBW resonant deposition location. In the ELM-free phases of the discharges where the density and thus the edge density gradient increase dramatically, the stray radiation (measuring the non-absorbed EC power) clearly decreases, indicating that high conversion efficiency is at stake. The diamagnetic loop signal (DML measuring the toroidal magnetic flux linked to the

total plasma energy) confirms that power absorption goes up to 60%. However the DMPX integrated signal is dominated by sawteeth (ST) perturbing the plasma centrally on a wide radius with a strong amplitude due to the low q and high I_p of the discharges. Moreover sawteeth have the tendency to lock to the heating modulation frequency and therefore prevent from using standard FFT analysis of the DMPX channels to determine a power deposition location at $\rho_\psi < 0.7$. A reliable quantity that can be compared from one channel to another to find the absorption location is the slope change of the soft X-ray time-traces due to a heat pulse injected between sawtooth crashes. The slope difference is calculated from linear fits of the 64 soft X-ray time-traces $0.5-2$ ms before and after the onset of the EC power pulse excluding the sawtooth crash high transport phase. (Fig. 3). The "slope-break" profile obtained is compared to the phase profile from the cross-correlation between the EC power pulse and the soft X-ray channels. The DMPX chords exhibiting both a maximum of slope change and a simultaneity with the power pulse indicate the radius of power deposition. Changing the magnetic field, this "slope-change" method applied to selected EC power pulses results in a deposition location shifted from the LFS ($\overline{\rho_{\rm vol}} \simeq 0.61$) to the HFS ($\overline{\rho_{\rm vol}} \simeq 0.51$) through the core of the plasma ($\overline{\rho_{\rm vol}} \simeq 0.15$) with decreasing B_φ (Fig. 4). The discrepancy between results from DMPX chords viewing in the HFS (negative $\rho_{\rm vol}$) and LFS (positive $\rho_{\rm vol}$) is very likely due to the integration of the signal along the lines of sight coupled to geometrical effects (positive triangularity of the plasma). ART simulations for those shots ($\triangle$ in Fig. 4) confirm that the absorption was moved from one side of the magnetic axis to the other, with two power deposition locations ($\triangle$ and $\triangledown$) for the high $B_\varphi = -1.49$ T.

Conclusion The presence of an optimum viewing angle together with the frequency dependence of the signal onset densities matching the O-mode cutoff densities assessed the attribution of the EC emission from overdense TCV plasmas to B-X-O EBE. Initial modulated power injections at the equator of H-mode plasmas allowed EBWH at different radii thus demonstrating EBW core deposition for the first time in TCV. The difficulties to localize the power deposition due to strong sawtooth activity in these experiments, linked to the need of low-q H-mode to generate steep density gradients, were overcome with a "slope-change" method applied to soft X-ray channels. Analysis of the DMPX inverted data as well as a comparison to several models are in progress in preparation of new experiments with continuous central EBW heating.
This work was partly funded by the *Fonds National Suisse de la Recherche Scientifique*.

---

[3] *Permanent address: EADS Deutschland, Defence and Security Systems, D-89077 Ulm*

References

[1] I.B. Bernstein, Phys. Rev. **109**, 10 (1958)

[2] J. Preinhaelter and V. Kopecký, J. Plasma Phys. **10**, 1 (1973)

[3] E. Mjølhus, J. Plasma Phys. **31**, 7 (1984)

[4] A. Mueck et al, Phys. Rev. Lett. **98**, 175004 (2007)

[5] T.P. Goodman et al, Fusion Sci. Technol., (in press). This conference.

[6] A.Yu. Popov and A.D. Piliya, Plasma Phys. Reports **33**, 109 (2007)